

## Uncertainty in determining interval velocities from surface reflection seismic data

Dan D. Kosloff\* and Yonadav Sudman\*

### ABSTRACT

The ability of reflection seismic data to uniquely determine the subsurface velocity has been uncertain. This paper uses a tomographic approach to study the resolution of typical seismic survey configurations. The analysis is first carried out in the spatial Fourier domain for the case of a single horizontal reflector. It is found that for a ratio of maximum offset to layer depth of one, the lateral resolution is very low for velocity and interface depth variations of wavelengths of approximately two-and-a-half times the layer thickness. The resolution improves with an increase in the ratio of maximum offset to layer depth. The results of the analysis in the Fourier domain are confirmed by results from a least-squares tomographic algorithm. It is found that regularization of the tomography by adding damping terms suppresses the spurious oscillations resulting from the areas of low resolution at the expense of loss of resolution at the shorter spatial wavelengths. Analysis of the single layer response for 3-D survey geometry shows that a 3-D acquisition with multi-azimuthal coverage has the potential to significantly improve velocity determination.

### INTRODUCTION

The determination of the subsurface velocity from seismic data is a fundamental part of seismic data processing and is a key to correct imaging of the earth's upper structure. Velocity analysis for depth imaging is more stringent than velocity analysis for typical time processing. Interval velocities used for depth processing honor a higher precision than the smoother stacking or rms velocities more appropriate for time processing. The resolving ability of reflection seismology to determine subsurface depth and velocity variations has been questioned, especially for structures containing layers with laterally varying velocity. The purpose of our paper is to examine this issue.

Several researchers have addressed the topic of the resolution of the seismic reflection method. Bube et al. (1995) showed that there are vertical variations in the velocity which do not produce changes in traveltimes. They concluded that these velocity variations cannot be uniquely determined from reflection seismic data. However, they claimed that the interface depths are resolvable. Their work implies that structures in which the layer velocities vary only laterally can be resolved both in terms of the velocity and of the interface depth. On the other hand, Bickel (1990), Sherwood et al. (1986), and Tieman (1994) reached a different conclusion: for such structures there is a range of wavelengths of the seismic velocities and interface depths for which a unique solution cannot be determined. Perhaps the difference between the conclusions of these investigators can be explained by the fact that Bube et al. (1995) referred to a strict null space, whereas Bickel (1990), and Sherwood et al., (1986) referred to very small but not necessarily zero eigenvalues.

Our paper reexamines the velocity determination problem using a tomographic approach. The subsurface models considered are layered structures where both the velocity and interface depth need to be determined. The velocity updates within each layer are constant in the vertical direction and laterally variant in the horizontal direction. Since the velocity determination issue is quite complicated, we use initial models which were sufficiently close to the correct models to ignore non-linear effects. An additional assumption used throughout our study is that both the initial models and the updated models should produce the same zero-offset traveltimes. This assumption is equivalent to the requirement that the models reproduce the time picks of layer reflections on a stacked common-midpoint (CMP) section. The fulfillment of this assumption, at least in an approximate sense, helps maintain physical feasibility and stability in velocity analysis in the depth domain by excluding models which produce zero-offset time picks which significantly deviate from the observed picks.

In order to make the study of uncertainty more tractable, we examine simple initial models containing horizontal layers

Manuscript received by the Editor September 29, 2000; revised manuscript received October 9, 2001.

\*Tel Aviv University, Department of Geophysics, P.O. Box 39040, Ramat Aviv, Tel Aviv 69978, Israel, and Paradigm Geophysical, Gav Yam 3, 9 Shenkar Street, Herzlia B 46120, Israel. E-mail: dan@paradigmgeo.com; yonadav@paradigmgeo.com.

© 2002 Society of Exploration Geophysicists. All rights reserved.

with uniform velocity. Since these models are spatially invariant, part of the analysis is carried out in the spatial Fourier domain. However, our conclusions also apply to laterally variant models.

The first section of this paper establishes the spatial discretization used in the study. Next, the tomographic equations for a single horizontal layer are derived in two dimensions in the spatial Fourier domain. The velocity resolution is examined for different offset-to-depth ratios. We found that, for the range of offset to depth ratios typically used in exploration geophysics, there are wavelengths of the velocity variation which are difficult to resolve. Subsequently, the analysis is carried out for 3-D acquisition geometry. We show that the velocity resolution improves when the 3-D survey contains a range of source-receiver azimuths. In the following sections, we investigate the solutions of a global tomographic scheme which was originally designed for nonhorizontal structures (Kosloff et al., 1996). This algorithm includes spatial discretization and uses damping terms for the stabilization of the solution. The results of the tomographic scheme agree with analysis in the Fourier domain and confirm the presence of velocity and interface depth variation that are difficult to determine.

### SPATIAL DISCRETIZATION

Our paper examines tomographic updates of initial models of horizontal layers with uniform velocity (Figure 1). Denoting by  $\delta t_h(x)$  the difference between the observed and calculated traveltime at a midpoint  $x$  and for a half offset  $h$ , the tomography searches for slowness and layer thickness updates  $[\delta s(x), \delta H(x)]$  which change the traveltime by this amount. The slowness and layer thickness updates within a layer are laterally variable but constant in the vertical direction. The updates are calculated at nodes which are horizontally separated by constant increments. The solution between nodes is calculated by linear interpolation from neighboring

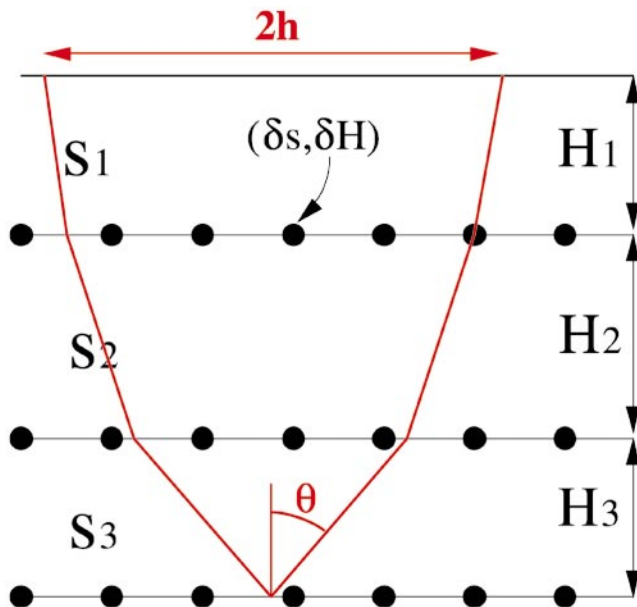


FIG. 1. Spatial discretization for slowness ( $S$ ) and layer thickness ( $H$ ) estimation.

nodes (we found that using higher order interpolation does not modify our conclusions).

In order to further constrain the velocity determination, we added the requirement that the initial model and the updated model produce equal zero-offset traveltimes. This important assumption is equivalent to the requirement that the zero-offset times from all models must closely match the traveltimes picks on a stacked CMP section. This constraint is used explicitly in the derivation in the next section. However, in the tomographic algorithm used in subsequent sections, the condition is applied as a “soft” constraint in the least-squares formulation.

### TOMOGRAPHIC RESPONSE OF A SINGLE HORIZONTAL LAYER

This section presents the tomographic response of a horizontal layer with uniform velocity.

Let  $H$  denote the layer thickness and  $s$  denote the layer slowness. The traveltime change  $\delta t_h(x)$  at the midpoint location  $x$  for a half-offset  $h$  resulting from slowness and layer thickness changes  $\delta s(x)$  and  $\delta H(x)$ , respectively, is given by

$$\delta t_h(x) = \frac{1}{\sin \theta_h} \int_{x-h}^{x+h} \delta s(x') dx' + 2s(x) \cos \theta_h \delta H(x), \quad (1)$$

where  $\sin \theta_h = h/\sqrt{h^2 + H^2}$ . This equation is a simplification of the tomographic principle for laterally variable models given in Farra and Madariaga (1988) and Kosloff et al. (1996). The equation is also equivalent to equations (1) and (2) in Bube et al. (1995), except that there the integration is carried out over the vertical coordinate. Our equation (1) is also similar to equation (37) in Bickel (1990), but he uses the velocity as a variable instead of the slowness. In the tomographic linearization, the first term is the integral of the slowness change along the raypath of the initial model, whereas the second term gives the contribution from the change in interface depth.

For laterally invariant models, equation (1) can be written as a spatial convolution:

$$\delta t_h(x) = \frac{1}{\sin \theta_h} \pi\left(\frac{x}{2h}\right) * \delta s(x) + 2 \cos \theta_h s(x) \delta H(x), \quad (2)$$

where  $*$  denotes a convolution and  $\pi(x)$  is the boxcar function

$$\pi(x) = \begin{cases} 1 & \text{for } |x| < 1/2 \\ 1/2 & \text{for } |x| = 1/2 \\ 0 & \text{for } |x| > 1/2 \end{cases},$$

and  $\delta(x)$  is the Kronecker delta.

After introducing time-normalized variables  $\delta s'(x) = H\delta s(x)$  and  $\delta H'(x) = s\delta H$ , the spatial Fourier transform of equation (2) yields

$$\delta \tilde{t}_h(k) = \frac{2}{\cos \theta_h} \text{sinc}(kh) \delta \tilde{s}'(k) + 2 \cos \theta_h \delta \tilde{H}'(k), \quad (3)$$

where  $\text{sinc}(x) = \sin(x)/x$ .

For models which conserve zero-offset time,

$$t_0 = 2sH = 2(s + \delta s)(H + \delta H),$$

with  $t_0$  the zero offset time. To first order,  $\delta s' = -\delta H'$ , and equation (3) becomes

$$\delta\tilde{t}_h(k) = \left( \frac{2}{\cos \theta_h} \text{sinc}(kh) - 2 \cos \theta_h \right) \delta\tilde{s}'(k). \quad (4)$$

This equation relates the spatial transform of the time error at a given offset to the transform of the slowness perturbation. In a multioffset experiment, the problem becomes overdetermined. The least-squares solution is;

$$\begin{aligned} & \sum_{h=h_{min}}^{h=h_{max}} \left( \frac{2}{\cos \theta_h} \text{sinc}(kh) - 2 \cos \theta_h \right)^2 \delta\tilde{s}'(k) \\ &= \sum_{h=h_{min}}^{h=h_{max}} \left( \frac{2}{\cos \theta_h} \text{sinc}(kh) - 2 \cos \theta_h \right) \delta\tilde{t}_h(k). \end{aligned}$$

The ability of the tomography to resolve a wavenumber component of the slowness variation depends on the sum on the left-hand side of the equation. Figure 2 plots

$$r = \sum_{h=h_{min}}^{h=h_{max}} \left( \frac{2}{\cos \theta_h} \text{sinc}(kh) - 2 \cos \theta_h \right)^2$$

as a function of the wavelength to layer-depth ratio (where  $\lambda/H = 2\pi/kH$ ) for  $h_{min} = 0$  and a maximum offset-to-depth ratio of one. The figure shows that the tomographic resolution is very low in the range of wavelengths around  $\lambda/H = 2.4$ . Interestingly, the resolution for the shorter wavelengths is very good. When the maximum offset-to-depth ratio is increased, the resolution slowly improves, and the point of minimum resolution shifts to longer wavelengths (Figure 3). However the resolution value at the minimum point remains low unless very large offset-to-depth ratios are present.

**EFFECT OF SPATIAL DISCRETIZATION AND INTERPOLATION**

The analysis of the previous section was for continuous slowness and layer thickness updates. A more complete evaluation needs to consider the effects of spatial sampling and interpolation.

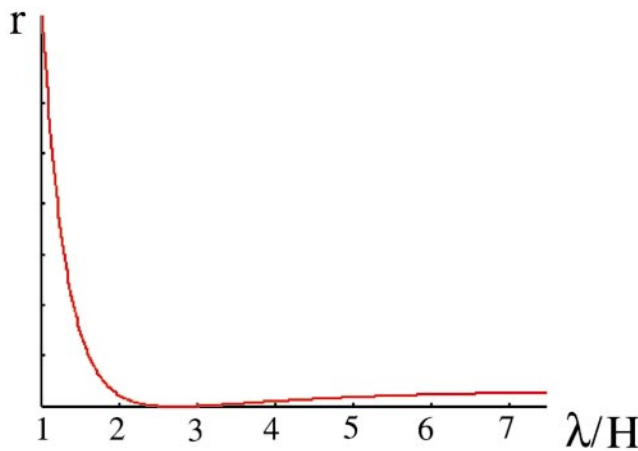


FIG. 2. Slowness resolution as a function of normalized wavelength for a single homogeneous layer with an offset-to-depth ratio of one.

When a function  $f(x)$  is linear interpolated from its sample values  $f(j dx)$ ,  $j = 0, \pm 1, \pm 2, \dots$ , with  $dx$  the sampling rate, the reconstruction can be written as a convolution,

$$f^{rec}(x) = \wedge \left( \frac{x}{dx} \right) * \sum_n \delta(x - n dx) f(n dx), \quad (5)$$

where  $f^{rec}(x)$  is the reconstruction of  $f(x)$  by interpolation, and  $\wedge(x)$  is the triangle function:

$$\wedge(x) = \begin{cases} 1 - |x| & \text{for } |x| \leq 1 \\ 0 & \text{for } |x| > 1 \end{cases}$$

A spatial Fourier transform of equation (5) yields

$$\tilde{f}^{rec}(k) = \text{sinc}^2 \frac{k dx}{2} \sum_{j=0}^{\infty} \tilde{f} \left( k + \frac{2\pi}{dx} j \right).$$

Using the relation in equation (4), where  $\delta s'^{rec}$  is substituted for  $\delta s'$  yields

$$\begin{aligned} \delta\tilde{t}_h(k) &= \left( \frac{2}{\cos \theta_h} \text{sinc}(kh) - 2 \cos \theta_h \right) \text{sinc}^2 \frac{k dx}{2} \\ &\times \sum_{j=0}^{\infty} \delta\tilde{s}' \left( k + \frac{2\pi}{dx} j \right). \end{aligned} \quad (6)$$

Equation (6) gives the discretized tomographic principle for a single horizontal layer. Figure 4 compares the discrete and the continuous tomographic least-squares responses for an offset-to-depth ratio of one and  $dx = H/2$ . The figure shows that response at the short wavelengths is highly attenuated by the interpolation. However, the long wavelength responses remains very similar to the continuous response. Use of a smaller spatial sampling rate would cause less attenuation of the shorter wavelengths. Conversely, it would appear that the instability caused by the spectral minimum can be avoided by selecting a spatial sampling rate greater than half the wavelength at the minimum. Figure 5 shows, however, in that case, the long wavelength response of the tomography differs from the continuous response. The best approach, therefore, seems to be to

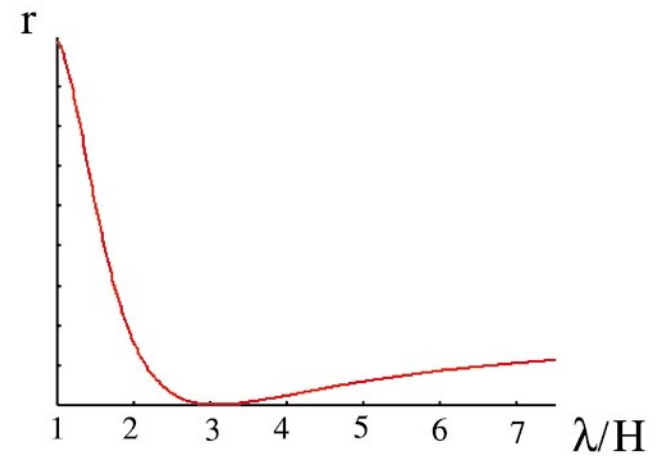


FIG. 3. Slowness resolution as a function of normalized wavelength for a single homogeneous layer with an offset-to-depth ratio of two.

use a spatial sampling rate which is smaller than half the wavelength of the spectral minimum and find an alternative strategy to handle the poorly determined part of the solution. A later section analyzes this topic.

#### TOMOGRAPHIC RESPONSE FOR 3-D SURVEY GEOMETRY

So far, the conclusions of this work have been for 2-D seismic acquisition. Three-dimensional acquisition can enable multiazimuthal ray coverage of the subsurface, which perhaps can reduce the uncertainty in the velocity determination. This section analyzes the tomographic response of a single uniform horizontal layer for 3-D acquisition.

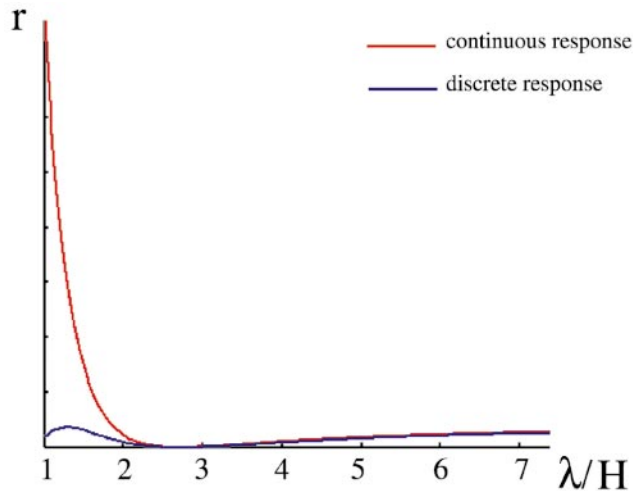


FIG. 4. A comparison between continuous and discrete showiness resolution for a single homogeneous layer with an offset-to-depth ratio of one and a spatial sampling equal to half the layer thickness.

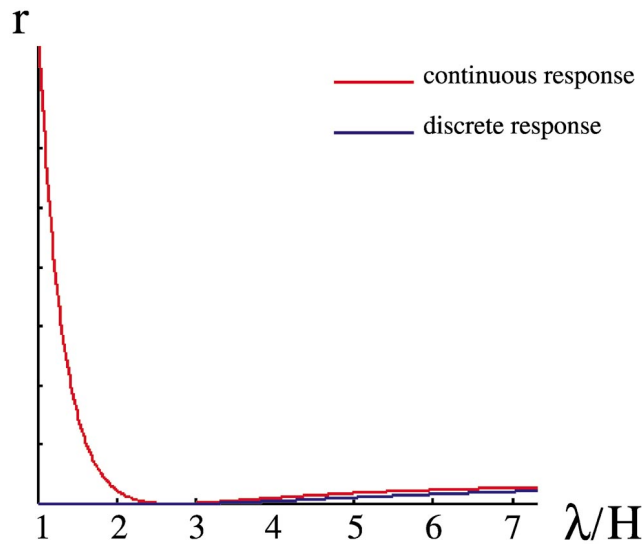


FIG. 5. A comparison between continuous and discrete showiness resolution for a single homogeneous layer with an offset-to-depth ratio of one and a spatial sampling equal to the layer thickness.

Let the  $x$  coordinate coincide with the in-line direction and the  $y$  coordinate coincide with the cross-line direction (Figure 6). For a shot-receiver pair with an azimuth  $\Psi$  from the in-line direction and with an offset  $2h$ , we separate the offset into an in-line half-offset  $h_x$  and a cross-line half-offset  $h_y$  according to  $h_x = h \cos \Psi$  and  $h_y = h \sin \Psi$  (Figure 6).

Let  $x'$  and  $y'$  denote a different coordinate system where  $x'$  coincides with the shot-receiver direction on the surface (Figure 6). Within this system, the tomographic response is obtained from the 2-D response (2) according to

$$\delta t_h(x', y') = \frac{1}{H \sin \theta_h} \pi \left( \frac{x'}{2h} \right) \delta(y') * \delta s'(x', y') + 2 \cos \theta_h \delta(x') \delta(y') * \delta H'(x', y'),$$

where  $*$  denotes a 2-D convolution.

Imposing the preservation of zero-offset time, transforming to the spatial wavenumber domain, and rotating the results to the original coordinate system yields

$$\tilde{\delta} t_h(k_x, k_y) = \left( \frac{2}{\cos \theta_h} \text{sinc}(k_x h_x + k_y h_y) - 2 \cos \theta_h \right) \times \tilde{\delta} s'(k_x, k_y).$$

The least-squares response becomes

$$r = \sum_{h_x, h_y} \left( \frac{2}{\cos \theta_h} \text{sinc}(k_x h_x + k_y h_y) - 2 \cos \theta_h \right)^2. \quad (7)$$

This result is first used for analyzing the velocity resolution of a 3-D marine survey with a single streamer. The layer depth  $H$

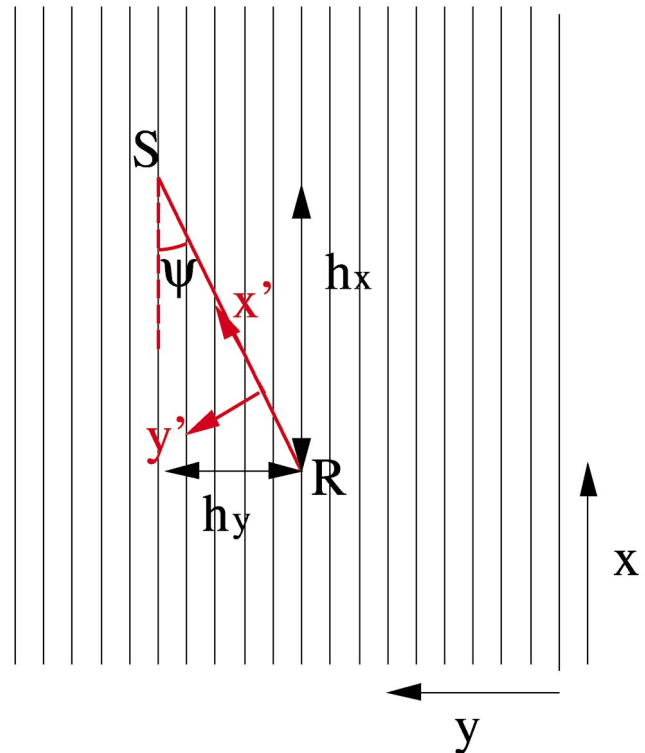


FIG. 6. Three-dimensional survey configuration.

was 1000 m, the minimum offset was 100 m, and the maximum offset was 1000 m. Figure 7 presents a color plot of the tomographic response as a function of the in-line ( $\lambda_x$ ) and cross-line ( $\lambda_y$ ) wavelengths of the slowness perturbation. The area of low resolution appears in the plot in red. Since the survey geometry contains only one azimuth, this result is two dimensional and similar to Figure 2.

The next test was a three-streamer survey. The distance between the streamers was 200 m in the cross-line direction. The remaining parameters were as in the previous example. The tomographic response shown in Figure 8 shows that in spite of

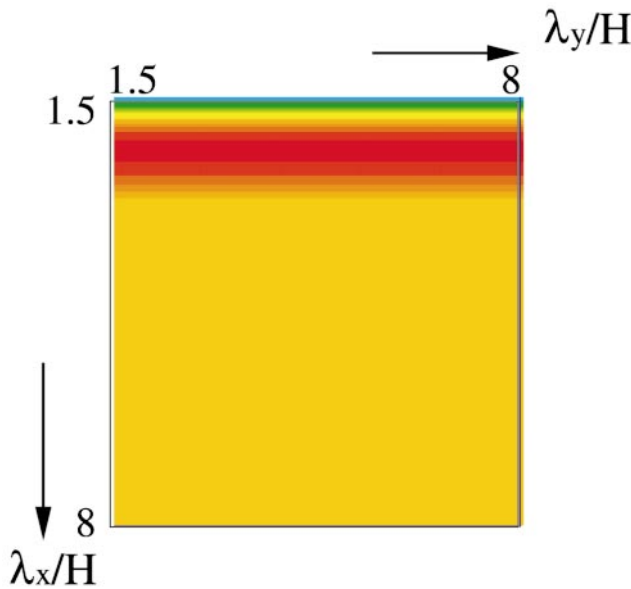


FIG. 7. Velocity resolution as a function of normalized in-line and cross-line wavelengths for a single streamer 3-D marine survey. Red = low resolution; green = high resolution.

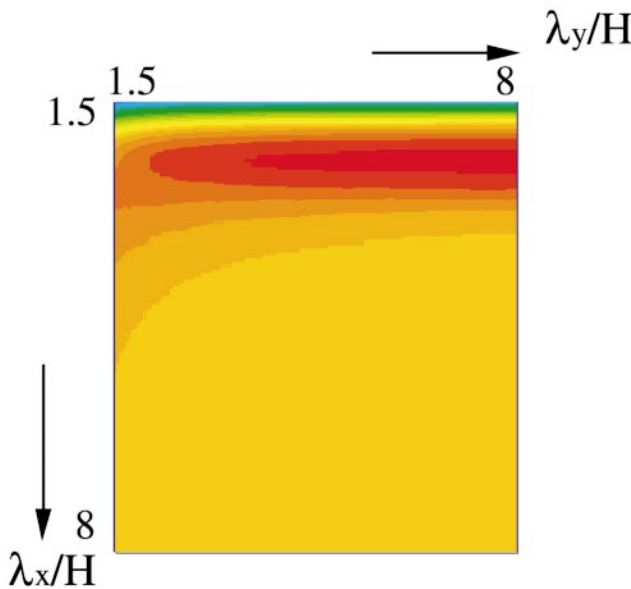


FIG. 8. Velocity resolution as a function of normalized in-line and cross-line wavelengths for a three-streamer 3-D marine survey. Red = low resolution; green = high resolution.

the fact that the azimuth range for the larger offsets is quite small in this example, the spectral minimum is shallower than in Figure 2 for the single streamer, especially in the in-line direction.

The third test was an equal distribution of offsets in the in-line and cross-line directions. The minimum and maximum offsets in both directions were 100 m and 1000 m, respectively. The response, shown in Figure 9, shows that the minimum has almost disappeared.

The conclusion from this section is that 3-D acquisition with a wide range of azimuths enables a much better determination of the velocity than with a 2-D acquisition. This can be understood by considering the example of a sinusoidal velocity variation in the  $x$  direction. If the wavelength of the variation is approximately equal to the wavelength of the spectral minimum of the 2-D resolution, the correct velocity cannot be recovered by acquisition with a single azimuth in the  $x$  direction. However, this velocity can be easily recovered with sufficient offsets in the cross-line  $y$  direction. It is important to note, however, that the time picking of the tomography needs to preserve the azimuthal information. The commonly used method of time picking by hyperbolic delay analysis usually ignores this part of the data (unless the analysis is divided into separate azimuth ranges). In tomography of depth-migrated data, the migrated gathers should be two dimensional with the output offsets defined in the in-line and cross-line directions.

**ADDING DAMPING TERMS TO THE TOMOGRAPHY**

Due to the presence of small eigenvalues, the least-squares solution of the tomography often becomes unstable. Stability can be restored by preconditioning the least-squares equations. This section evaluates the response of the tomographic algorithm described in Kosloff et al. (1996) which was originally designed for laterally variable structures. The tomographic

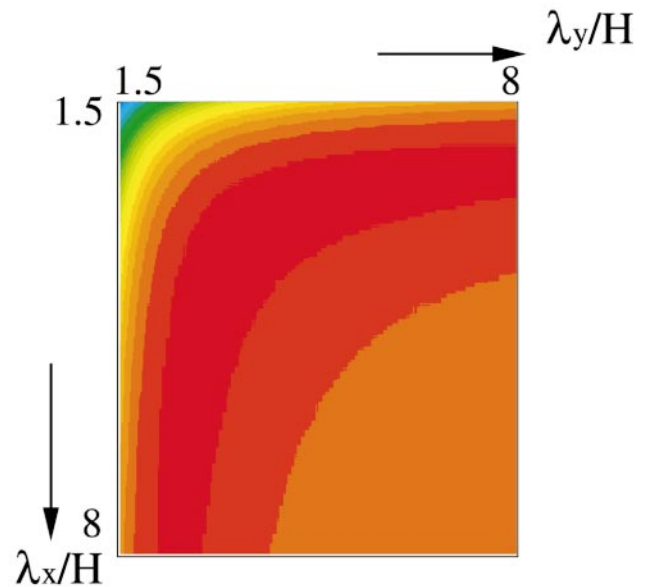


FIG. 9. Velocity resolution as a function of normalized in-line and cross-line wavelengths for a 3-D survey with a maximum offset-to-depth ratio of one and an equal distribution of azimuths in all directions. Red = low resolution; green = high resolution.

solutions are compared to the predictions of the analyses of the previous sections.

The numerical scheme uses the same spatial discretization shown in Figure 1; however, slowness and vertical time are used as the main variables, instead of slowness and layer thickness. The vertical time of the  $j$ th layer is related to the slownesses and thicknesses by (Kosloff et al., 1996)

$$t_v^j = 2 \sum_{i=1}^j s^i H^i.$$

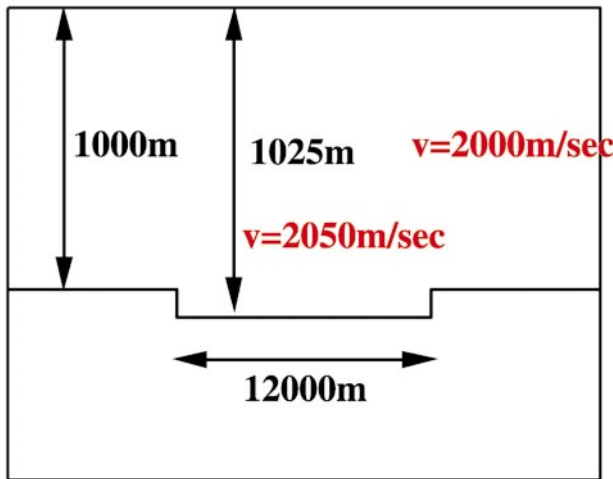


FIG. 10. Model configuration for the single-layer test.

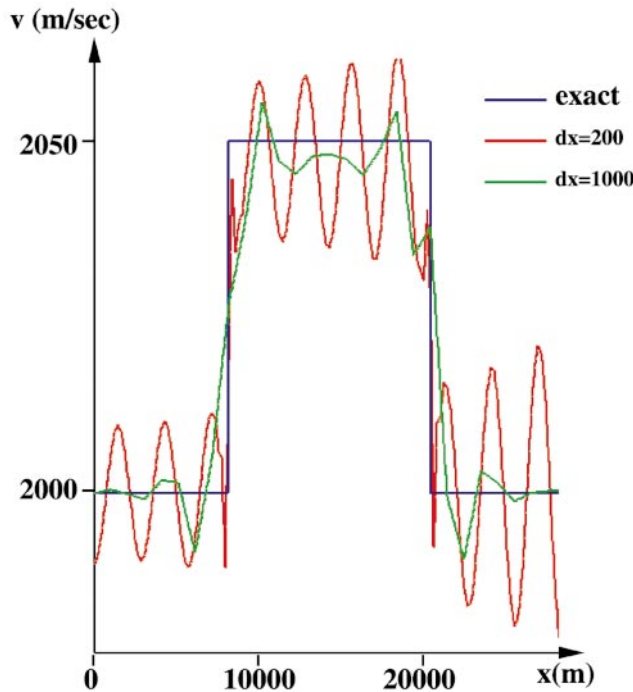


FIG. 11. Comparison between the exact solution and the calculated solution for the single-layer test without data regularization.

We have found that it is advantageous to work with the vertical time, instead of the time-normalized layer thickness, because in most cases it changes very little (for horizontal layers, the vertical time is equal to the zero-offset time, which is assumed constant in this study). By using the vertical time, instead of being a two-parameter problem, the tomography almost becomes a one-parameter problem.

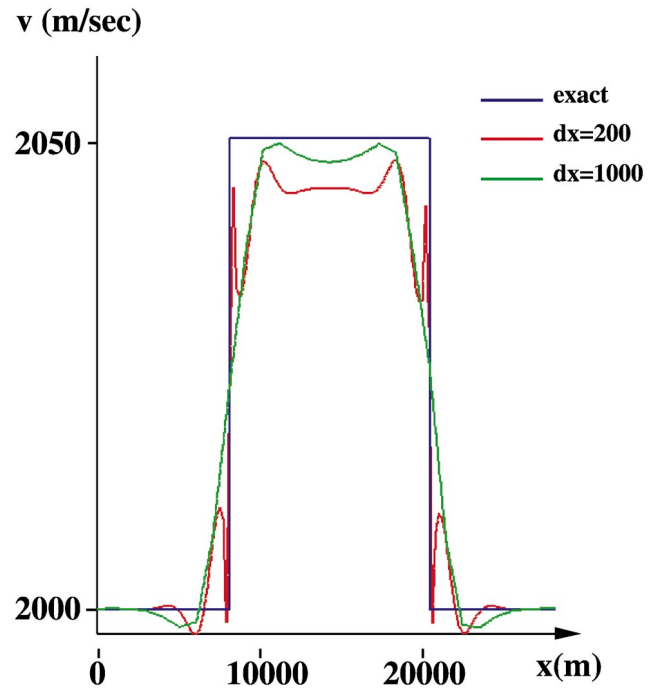


FIG. 12. Comparison between the exact solution and the calculated solution for the single-layer test with data regularization.

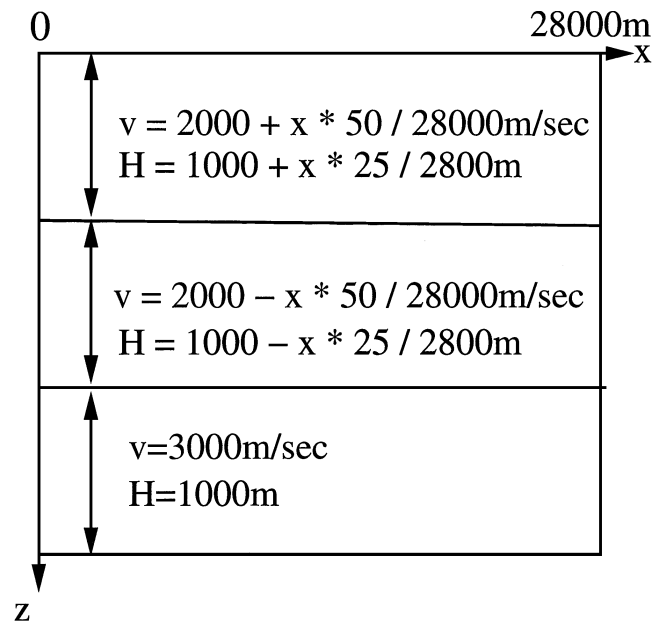


FIG. 13. Model configuration for the multilayer test with smooth velocity variation.

Let  $\delta\mathbf{m}$  denote vector of update parameters consisting of the slowness change  $\delta s$  and vertical time change  $\delta t_v$  at all the interpolation nodes. The discretized relation between model perturbations and the resulting traveltimes changes is

$$\delta\mathbf{t} = \mathbf{A}\delta\mathbf{m}, \quad (8)$$

where  $\delta\mathbf{t}$  is the data vector of travel time errors and  $\mathbf{A}$  is the influence matrix. The damped weighted least-squares solution of equation (8) is given by

$$(\mathbf{A}^T\mathbf{C}_D^{-1}\mathbf{A} + \mathbf{C}_M^{-1})\delta\mathbf{m} = \mathbf{A}^T\mathbf{C}_D^{-1}\delta\mathbf{t}, \quad (9)$$

where  $\mathbf{C}_D$  is the data covariance matrix containing the variance of the data on its diagonal, and  $\mathbf{C}_M$  is the parameter covariance matrix (Kosloff et al., 1996). Two types of regularization are considered, namely diagonal damping with the model variance, and second-derivative stabilization by adding a component of the  $(-1, 2, -1)$  convolution operator to  $\mathbf{C}_M$ . For the example of the single horizontal layer of the previous sections,

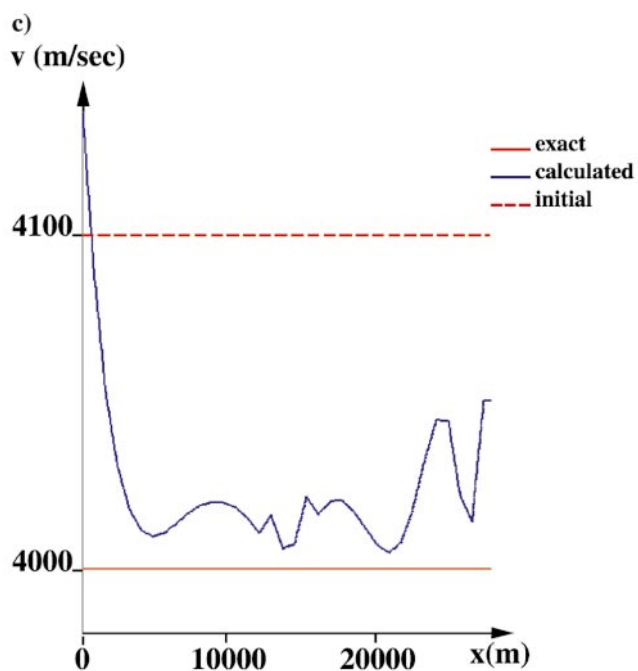
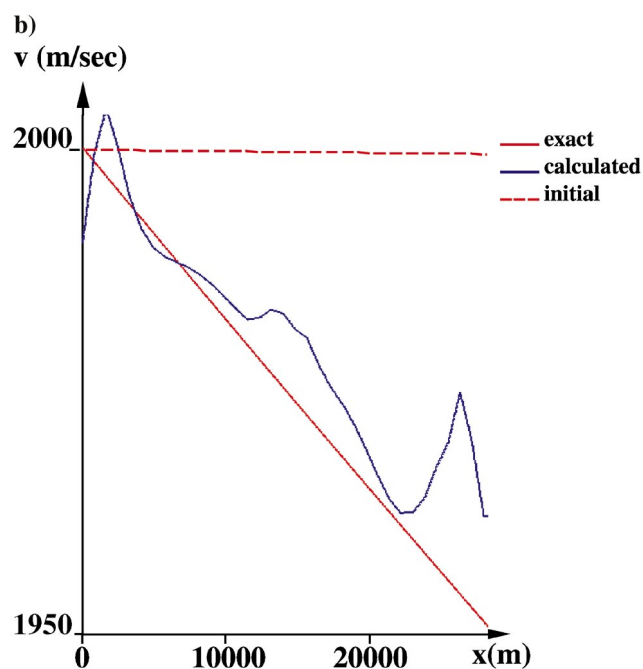
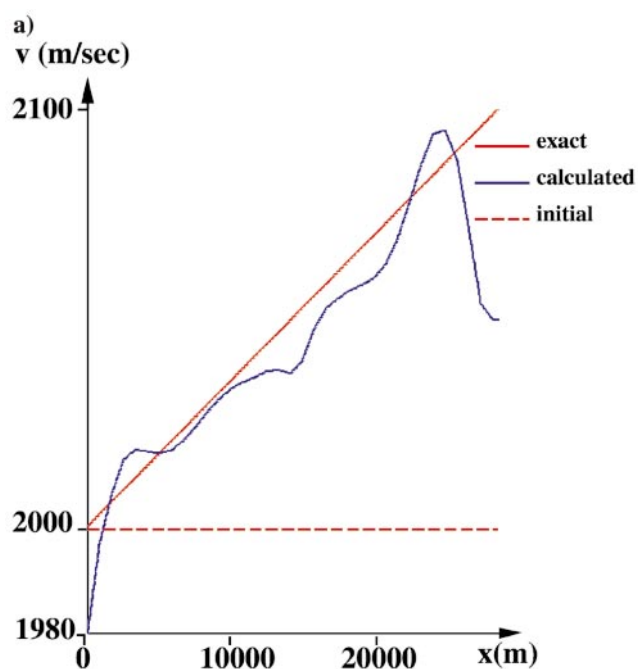


FIG. 14. Comparison between the exact solution and the calculated solution for the three-layer model with lateral-velocity and layer-thickness gradients. (a) First layer, (b) second layer, (c) third layer.

uniform diagonal damping raises the response by a fixed amount for all the wavelengths, while the second-derivative regularization decays like  $k^2$  for the small wavenumbers (or long wavelengths). It would appear that the second-derivative regularization should be the preferred method because it can be tailored to influence only the wavenumber components close to the spectral minimum of the tomographic response. However, we have found that it is difficult to predict the point of minimum response for the general case of nonhorizontal layers and, therefore, both types of conditioning are needed.

The tomographic scheme of Kosloff et al. (1996) was tested with a single horizontal-layer example. The tomography boundary conditions were of a constant update off the ends of the model. Preservation of zero-offset times was introduced through an additional term in the least-squares functional. The correct model contained a rectangular velocity and depth anomaly (Figure 10), where the zero-offset reflection time was equal to 1 s at all CMP locations. The offset range of the forward modeling was between 100 m and 1000 m, which is also the layer depth. The initial model consisted of a uniform layer of depth 1000 m and a velocity of 2000 m/s.

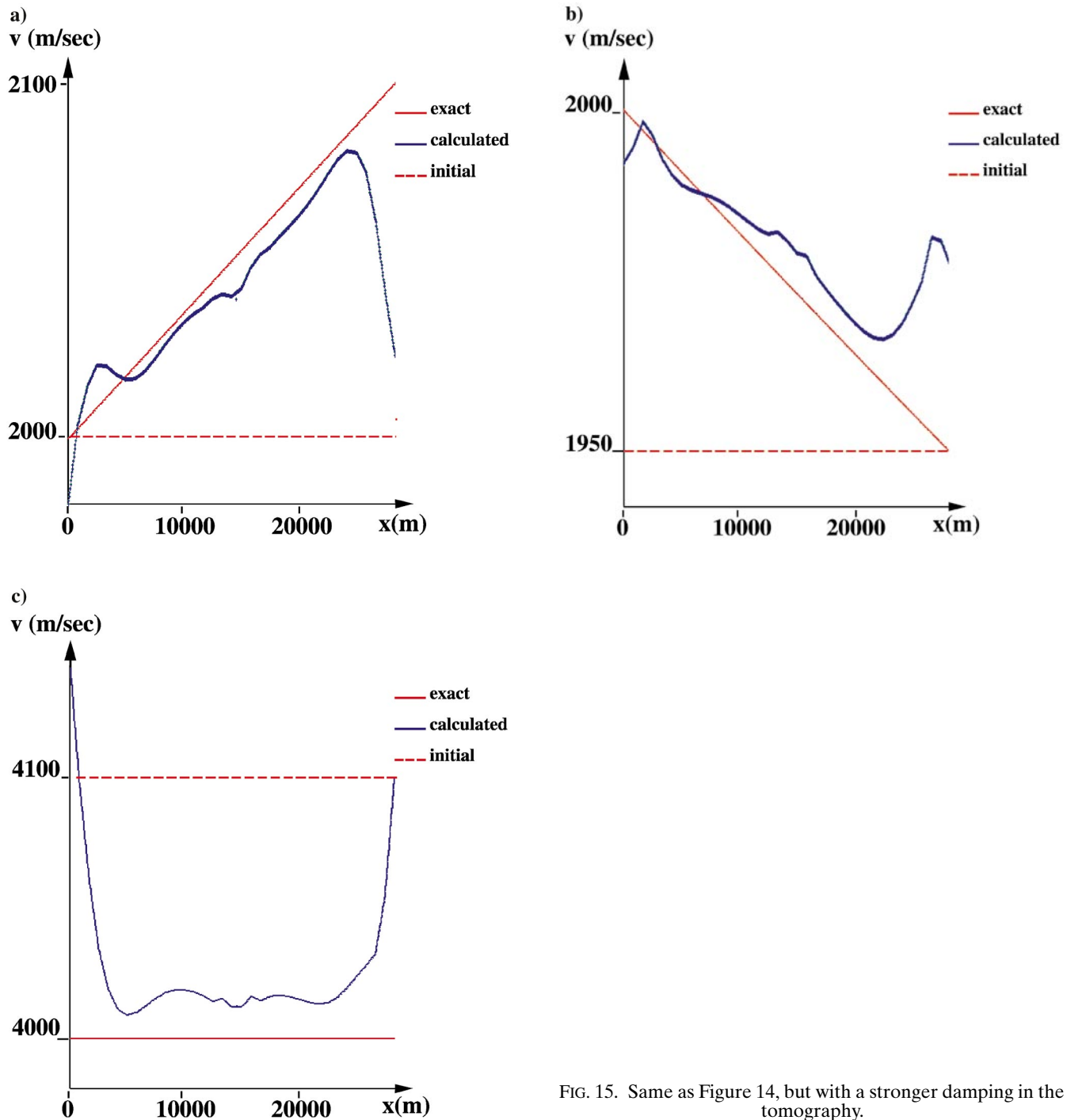


FIG. 15. Same as Figure 14, but with a stronger damping in the tomography.

At first, the tomography was run without preconditioning with an update node spacing  $dx$  of 200 m. A comparison between the correct velocity and the reconstructed velocity is shown in Figure 11. The figure shows that the tomography was able to obtain the main feature of the anomaly. However, the solution contains an oscillation. Interestingly, the oscillation wavelength is about 2400 m, which coincides with the predicted wavelength of the spectral minimum in the analysis of the previous section (Figure 5). When the update node spacing was increased to  $dx = 2000$  m, the tomographic solution became smoother, although it undershot and overshot the correct result (Figure 11).

In the second stage, the single-layer test was repeated using the same parameters except that diagonal and second-derivative preconditioning were added. The magnitude of the preconditioning was determined empirically. Figure 12 compares the exact solution to the calculated solution for  $dx = 200$  m and  $dx = 1000$  m. As the figure shows, the preconditioning suppressed most of the oscillation. However, as expected, some of the short-wavelength components of the solution are missing. Further tests have indicated that the values of the preconditioning parameters used in this example enable comparable results to be obtained for interpolation node separations within the range of  $dx = 200$  m and  $dx = 1000$  m. Similar values of the preconditioning parameters were used in the examples in the following sections.

#### THE MULTILAYER CASE

For structures containing more than one layer, there are more combinations of the velocities and layer thicknesses which are difficult to resolve. This section evaluates the resolution for two models, each of which contained three layers. The first model had a smooth velocity and layer thickness variations, whereas the second model contained isolated anomalies. The tomographic algorithm of Kosloff et al. (1996) was used in the tests.

In the first example (Figure 13), the velocity in the first layer varied linearly between 2050 and 2000 m/s, and the layer thickness varied linearly between 1025 and 1000 m. The velocity in the second layer varied linearly between 2000 and 1950 m/s, and the thickness varied linearly between 1000 and 975 m. The velocity for the third layer was constant and equal to 4000 m/s, and the interface depth was 3000 m. The initial model contained constant velocities in the three layers of 2000, 2000, and 4100 m/s, respectively, and constant thicknesses of 1000, 1000, and 1050 m, respectively. The offset-to-depth ratio in this example was the one for three layers.

The tomographically reconstructed velocities for the three layers are compared to the exact velocities in Figure 14. Figures 14a and 14b for the first two layers show that starting from an initial model with constant velocity, the tomography was able to obtain the gradient in the velocity variation. The discrepancy between the reconstruction and the exact model can be attributed to edge effects, particularly for the deeper layers and large offsets. For the third layer, the tomography was able to bring down the initial velocity of 4100 m/s closer to the correct value of 4000 m/s. However, the solution contains small oscillations ( $\pm 20$  m/s), and the velocity is slightly above the correct value. An increase in the damping of the tomography suppresses the oscillations to some degree. For

example, Figure 15 presents results using the same parameters as above except that the second-derivative smoothing term was strengthened by a factor of four. The results show smaller oscillations and appear superior to those in Figure 14. However, when using the stronger smoothing with models containing localized velocity anomalies, the response became overdamped. As expected, there appears to be a clear trade-off between resolution and smoothness.

The second multilayer example contained localized rectangular velocity and depth anomalies in the first two layers, and a uniform velocity in the third layer (Figure 16). The initial model contained horizontal layers of respective thicknesses of 1000, 500, and 1025 m, and velocities of 2000, 3000, and 4100 m/s, respectively. The forward modeling calculations were for an offset-to-depth ratio of one for the three layers. The tomographically updated velocities for the three layers are compared to the exact values in Figures 17a–c. The Figures show that the tomography was able to find the anomalies in the first two layers and was also able to bring the velocity in the third layer close to the correct value. However, as in the previous example, there are spurious oscillations.

An alternative approach to velocity analysis is to perform the velocity updating in a layer stripping fashion, where first, using the reflection data from the first layer, the velocity and layer thickness for that layer are found. In the second stage, the parameters of the second layer are found from its reflections while keeping to determined parameters of the first layer fixed. The process is then continued until all the layers of the model have been determined. The results from the analysis of a

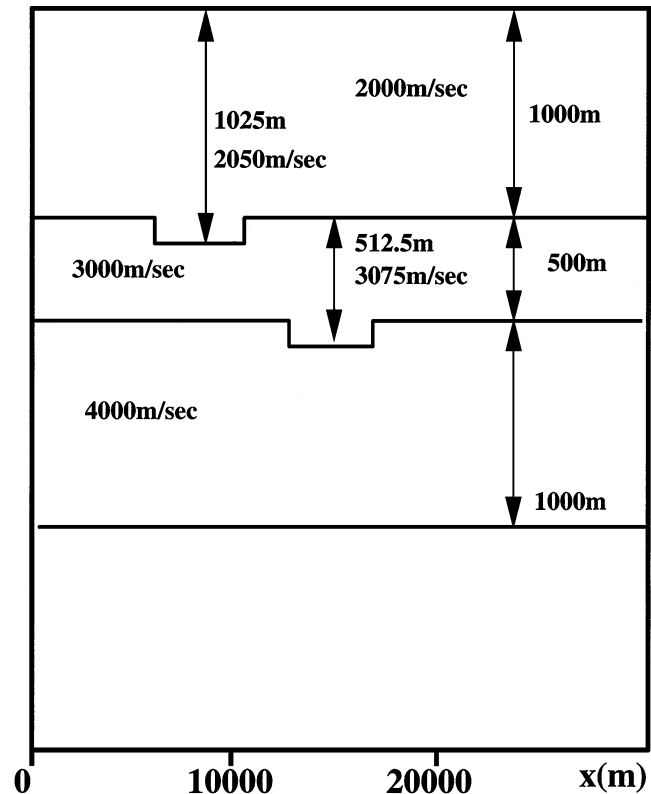


FIG. 16. Model configuration for the three-layer example with localized anomalies.

single-layer response apply for the evaluation of each step of the process. It may seem that because the response of a single layer is simpler than the multilayer response, this process would be more accurate. However, repeating the velocity determination for the previous example using layer stripping shows that

although the determined velocity for the first layer appears somewhat smoother (Figure 18a), the determined velocity for the second and third layers show the same type of oscillations which were present in the previous results. Moreover, the results for the third layer (Figure 18c) are worse than the

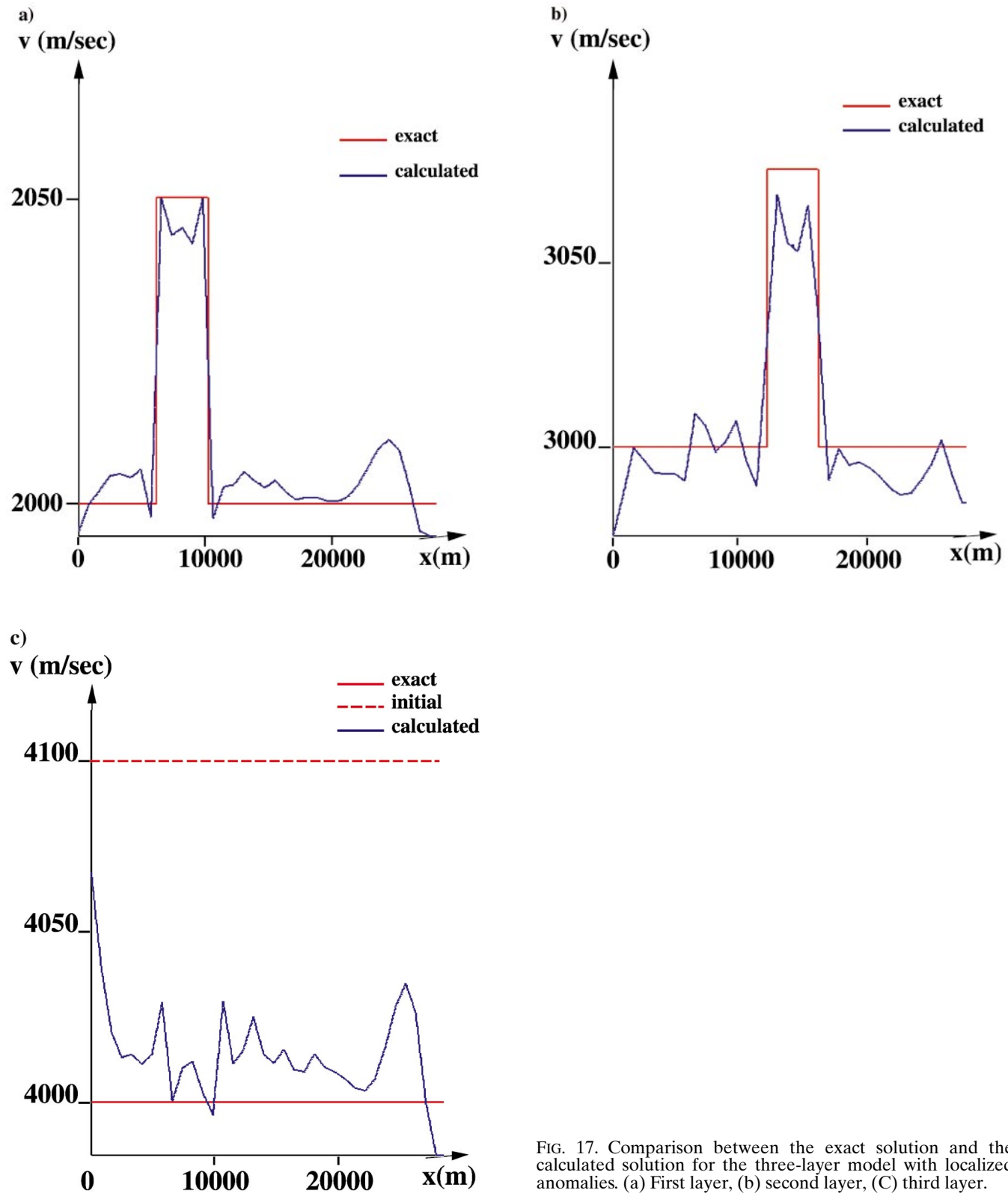


FIG. 17. Comparison between the exact solution and the calculated solution for the three-layer model with localized anomalies. (a) First layer, (b) second layer, (C) third layer.

results of the velocity determination without layer stripping. Furthermore, in many cases in real data, some of the shallow reflections are of low quality. Layer stripping then encounters further problems. The advantage of the nonlayer-stripping procedure is that part of the velocity determination of the shallow layers is done from the reflections from the deeper horizons.

### CONCLUSIONS

This work has shown that there are components of the slowness and interface depth variations which are difficult to resolve with typical reflection seismology experiments. The analysis of

the response of a single horizontal layer in the Fourier domain indicates that, with a maximum offset-to-layer-thickness ratio of one, it is very difficult to determine variations of the subsurface parameters in the range of wavelengths around 2.4 layer thicknesses. When the maximum offset is increased, the resolution slowly improves, and the wavelength at the point of minimum resolution increases. However, very long offsets are required to obtain good resolution at all wavelengths. For a maximum offset-to-layer-thickness less than one, the ability to resolve lateral variations in velocity becomes very questionable. These results qualitatively agree with the results of Bickel (1990). Lack of resolution manifests itself in the

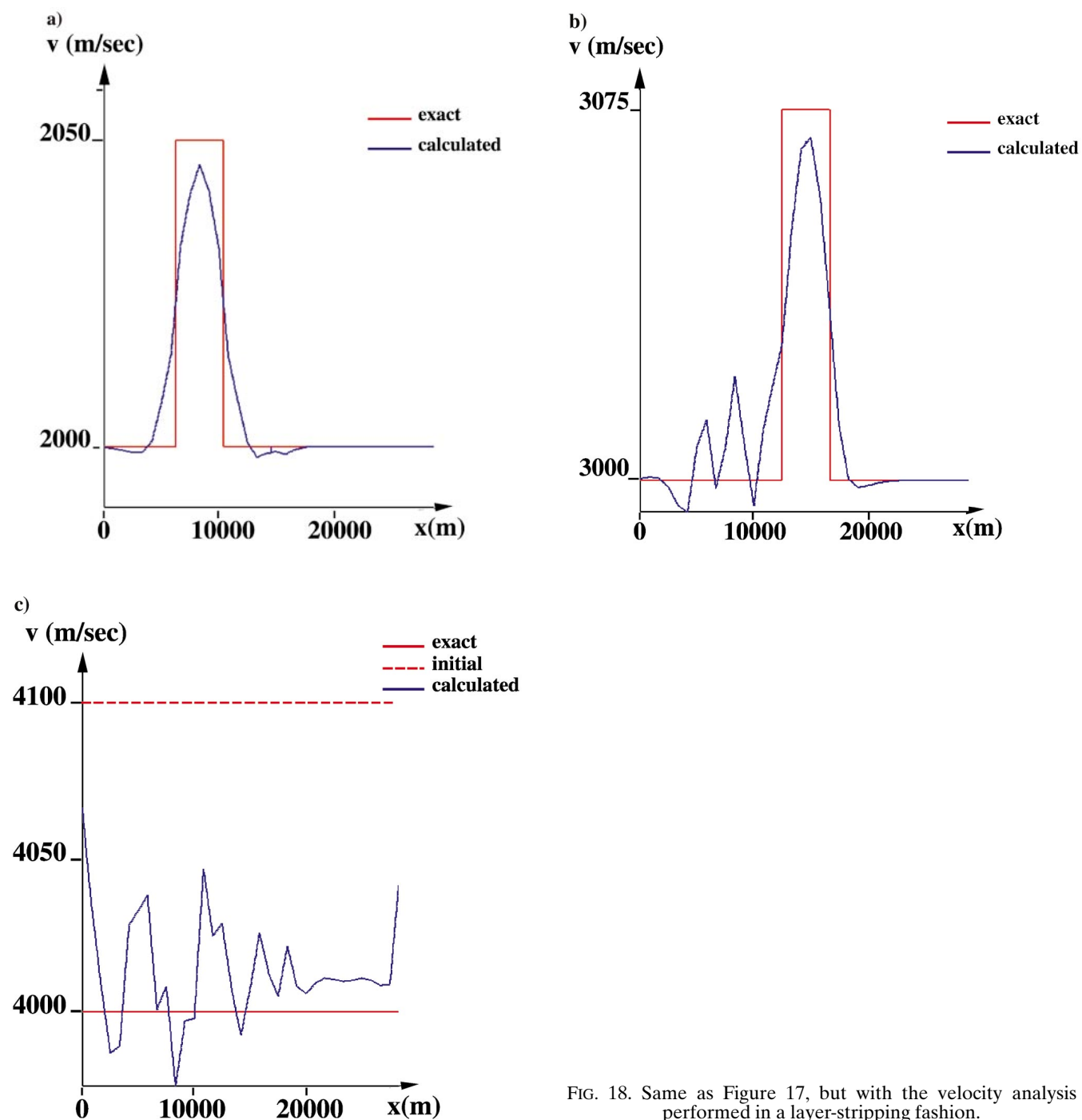


FIG. 18. Same as Figure 17, but with the velocity analysis performed in a layer-stripping fashion.

presence of different subsurface models which explain the seismic data equally well.

The single horizontal layer response was also analyzed using a least-squares tomographic scheme, originally designed for nonhorizontal layers. Although this method differs from the analysis in the Fourier domain, test results showed that when no preconditioning is applied, the tomographic reconstruction contains oscillations which have similar wavelengths to the wavelength of the spectral minimum predicted by the Fourier domain analysis. The addition of regularization to the tomography suppresses the oscillations at the expense of reduced resolution at the shorter wavelengths.

The tomographic scheme was applied to multilayered structures. Using horizontal initial models, we showed that the tomography with the selected regularization parameters was able to recover the main features of subsurface anomalies. However the solution contained some spurious noise which could only be reduced at the expense of lowering the resolution. The conclusion from these tests is that, with reflection seismology, only the long wavelengths of the subsurface velocity variation can be recovered with confidence. It is anticipated that these conclusions will be further strengthened when dealing with strongly laterally varying structures, where one can anticipate the presence of other wavelength components with low resolution. We believe that the results of this work apply to all methods of velocity analysis from reflection data, and they are not limited to the tomographic approach applied in this study. Moreover, single-station analysis methods, such as hyperbolic analysis, should have further difficulties since they do not account correctly for the variation of the velocity in the vicinity of the analysis point.

We showed that performing the velocity analysis in a layer-stripping fashion holds no significant advantages. Moreover layer stripping may produce inferior results for the deeper layers. However, this work was concerned with small velocity errors when the linearization of the tomography is valid. For

larger velocity and interface depth errors, it may be advantageous to first determine the parameters in the shallow part of the structure and then proceed to the deeper part. However, in such a case, while determining the parameters of the deeper layers, we still recommend allowing the parameters of the shallow part of the section to change.

Analysis of the single-layer response suggests that 3-D acquisition with multiazimuthal coverage has the potential to significantly improve velocity and interface depth determination. However, it is important to process the data in a manner which preserves the azimuthal information.

Finally, to end the discussion on a more optimistic note, we speculate that since the low-resolution parameter variations are limited to specific wavelength components, the incorporation of other data or of prior geologic knowledge may eliminate the uncertainty in the subsurface parameter determination.

#### ACKNOWLEDGMENT

The authors thank Zvi Koren for numerous helpful discussions.

#### REFERENCES

- Bickel, S. H., 1990, Velocity-depth ambiguity of reflection travel times: *Geophysics*, **55**, 718–729.
- Bube, K. P., Langan, R. T., and Resnick, R. R., 1995, Theoretical and numerical issues in the determination of reflector depths in seismic reflection tomography: *J. Geophys. Res.*, **100**, no. B7, 12449–12458.
- Farra, V., and Madariaga, R., 1988, Nonlinear reflection tomography: *Geophys. J. Internat.*, **95**, 135–147.
- Kosloff, D., Sherwood, J. W. C., Koren, Z., Machet, E., and Falkovitz, Y., 1996, Velocity and interface depth determination by tomography of depth migrated gathers: *Geophysics*, **61**, 1511–1523.
- Sherwood, J. W. C., Chen, K. C., and Wood, M., 1986, Depth and interval velocities from seismic reflection data for low relief structures: 18th Ann. Offshore Tech. Conf.
- Tieman, H., J., 1994, Investigating the depth-velocity ambiguity of reflection traveltimes: *Geophysics*, **59**, 1763–1773.